FESC FINAL PROJECT REPORT

Development of Novel Water Splitting Catalysts for the Production of Renewable Hydrogen

P.I. Helena Hagelin-Weaver
Department of Chemical Engineering
University of Florida

Project Time Period: 08/16/2011 – 06/30/2013

Executive Summary

The production of hydrogen from water using only solar energy is a promising pathway to the production of hydrogen from renewable energy sources and this process is particularly well-suited for Florida, the "Sunshine State".   As hydrogen is difficult to transport and store, producing hydrogen on site, in the State of Florida, for power plants which generate electricity using proton exchange membrane (PEM) fuel cells or internal combustion engines is particularly attractive.   Furthermore, hydrogen produced in this manner can be used in the production of chemicals, such as liquid fuels.   For example, "solar hydrogen" can be used to supplement synthesis gas (a mixture of hydrogen and carbon monoxide) derived from biomass (an abundant renewable fuel source in the State of Florida) to obtain the optimal 2:1 ratio of H_2:CO for Fischer-Tropsch synthesis of liquid hydrocarbon fuels, in particular diesel.   Fischer-Tropsch diesel can not only replace petroleum-based diesel and reduce Florida's and the Nation's dependence on foreign oil, it is also a very high quality diesel which will result in reduced emissions of NO_x and SO_x.

In this project a two-step thermochemical cycle was used in which water is passed over a reduced iron oxide catalyst to generate hydrogen while the oxygen is taken up by the oxygen-deficient iron oxide (Figure 1).   In the second step the resulting iron oxide is heated to desorb (release) the oxygen and regenerate the oxygen-deficient iron oxide to close the catalytic cycle. The key to a successful process is to develop catalytically active materials that can withstand temperatures up to 1500°C.   Our approach to catalyst development is to use zirconia, a high-temperature ceramic, as support for the iron oxide, and investigate the activity and stability of these catalysts over several oxidation-reduction cycles.
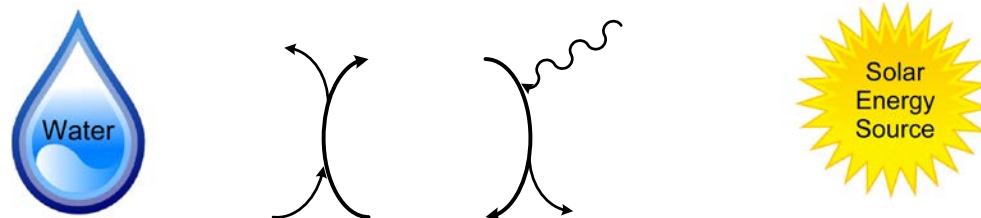

Figure 1. Two-step thermochemical cycle using iron oxide.

The effects of two zirconia supports, a nanoparticle zirconia (n-ZrO_2) and an yttria-stabilized zirconia with 8 mol% of yttria (8-YSZ), on the activity and stability of iron oxide-based catalysts were investigated as part of this research. The loading of iron was also varied to determine the optimal amount of iron oxide to be used in these reactions. The hydrogen evolution over these catalysts is presented for selected cycles in Figure 2. The higher hydrogen yield in the first step reveals that the catalyst is not stable after the activation step. However, after the second cycle, the most stable catalysts exhibit only a slight decrease in hydrogen yield with increasing cycle number. From the figure it is evident that the catalysts containing 20 weight % (wt%) iron are not as stable as the catalysts containing 10 wt% iron. While higher iron loadings are desirable to keep a high activity, at an iron loading of 20 wt% it appears that the iron is not sufficiently stabilized by the zirconia support.   The support is very important in this reaction and the behavior of the catalysts supported on n-ZrO_2 and the 8-YSZ are different (Figure 2). The 10-FeOx/n-ZrO_2 appears to be the most stable catalyst, while the 10-FeOx/8-YSZ has one of the highest initial hydrogen yields. However, since the hydrogen yield decreases more significantly

2

with each catalytic cycle for the 10-FeOx/8-YSZ, the hydrogen yield after ten cycles are similar on this and the 10-FeOx/n-ZrO$_2$ catalysts. Recent results reveal that the 15-FeOx/n-ZrO$_2$ catalyst (with an iron loading of 15 wt%) is a promising catalyst that warrants further investigation.
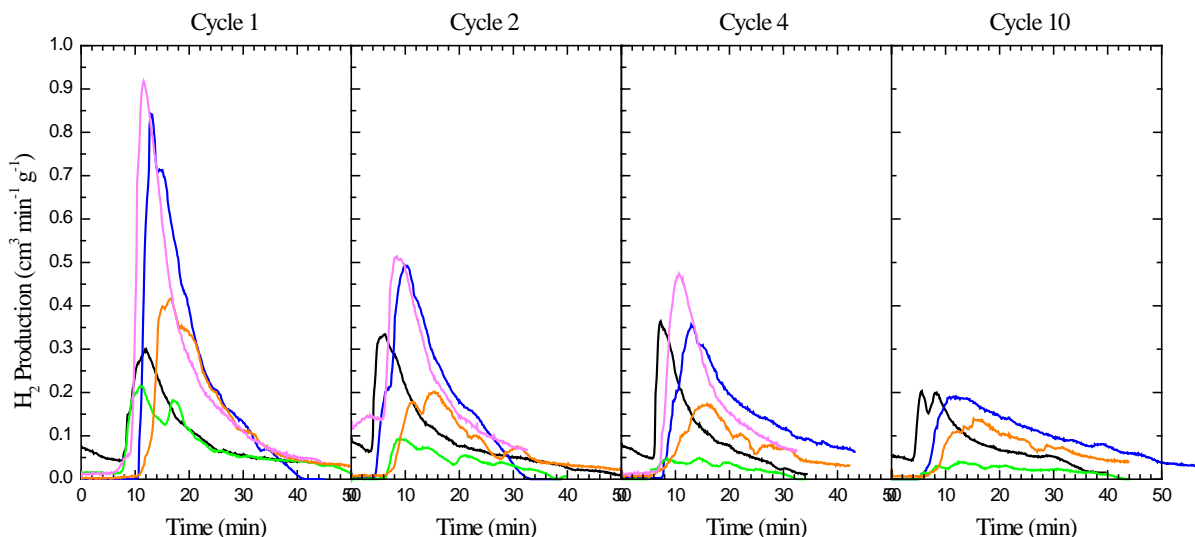

Figure 2. Hydrogen production at 1000 °C over different iron oxide catalysts supported on zirconia and yttria-stabilized zirconia. ——— 10wt% FeO$_x$/n-ZrO$_2$, ——— 15wt% FeO$_x$/n-ZrO$_2$, ——— 20wt% FeO$_x$/n-ZrO$_2$, ——— 10wt% FeO$_x$/8-YSZ, ——— 20wt% FeO$_x$/8-YSZ.

Careful catalyst characterization reveals that the surface areas of these catalysts are significantly reduced after reaction. This is expected due to sintering (particle growth) at the high reaction temperatures. However, the decrease in surface area from ~10 m^2/g to 1.5 m^2/g is not as severe as would have been expected for a nanoparticle catalyst exposed to these high temperatures. X-ray diffraction (XRD) data further supports this conclusion. While some increase in crystal size is observed after reaction (evident as more intense and sharper peaks in the XRD patterns), the differences in the XRD peak intensities between fresh and spent catalysts are not significant for the 10-FeOx/n-ZrO$_2$ catalysts (Figure 3). In contrast, the peaks due to the 8-YSZ support are more intense on the spent catalyst compared to the fresh (indicating particle growth during reaction), but the peaks due to iron oxide have also disappeared which indicates that the iron has been incorporated in the YSZ lattice. The iron does not enter the zirconia lattice of the n-ZrO$_2$-supported catalysts, and Fe$_3$O$_4$
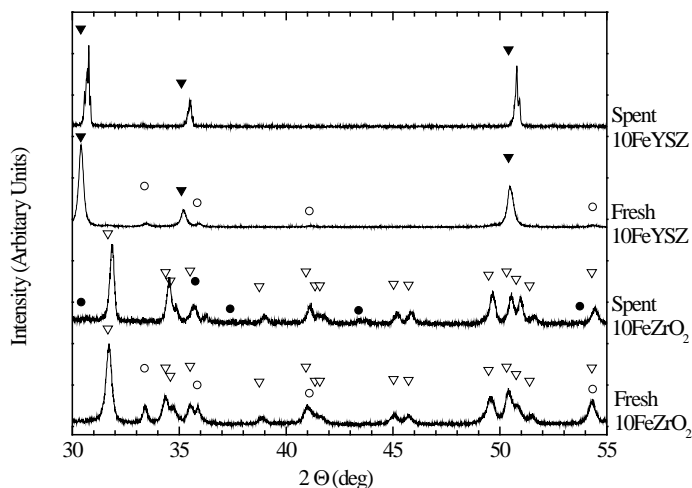

Figure 3. XRD spectra obtained from iron oxide precipitated on n-ZrO$_2$ and 8-YSZ. $\triangledown$ ZrO$_2$ (monoclinic), $\blacktriangledown$ YSZ (cubic), $\circ$ Fe$_2$O$_3$, $\newcommand{\x}{}$ ⬣ Fe$_3$O$_4$.

crystallites are visible is the XRD pattern obtained from the spent catalysts after the water-splitting reaction (the fresh catalysts consist of Fe_2O_3 before activation).

The results from this research indicate that iron-zirconia is a promising system that warrants further investigation, and the effects of other metal oxides are currently under investigation.

Table of Contents

Summary

A reactor system for the thermochemical splitting of water was designed and built as part of this project. Two types of catalysts were evaluated in this reactor system, iron oxide supported on nanoparticle zirconia ($FeO_x/n\text{-}ZrO_x$) and iron oxide supported on yttria-stabilized (8 mol%) zirconia ($FeO_x/8\text{-}YSZ$). In addition to the two supports, the effect of iron loading was also investigated between 10 % and 20 % of iron by weight. The two zirconia supports yield very different results. The iron supported on the 8-YSZ gives a higher initial hydrogen yield per cycle, but the decrease in yield with increasing cycle number is higher for this catalyst compared with the $FeO_x/n\text{-}ZrO_x$ catalyst. The $FeO_x/n\text{-}ZrO_x$ with a 10 wt% iron loading exhibited the most stable hydrogen yield during the ten cycles. At iron loadings of 20 wt% a significant deactivation is observed with increasing number of cycles. Apparently, this loading is too high for sufficient stabilization from the zirconia support. Initial results on a 15 wt% $FeO_x/n\text{-}ZrO_x$ catalyst are very promising, and this catalyst is currently under investigation.

Goals and Objectives

The goals of this project were two-fold; 1) develop catalytic materials that are stable up to temperatures of 1500°C and have reasonable catalytic activity for more than one cycle and 2) develop mixed metal oxide combinations that will release oxygen at temperatures lower than 1500°C (Step 2), while still maintaining water-splitting activity (Step 1). Iron oxide was chosen as the metal oxide since iron has several stable oxidation states and has been shown to have water-splitting activity, i.e. can remove oxygen from water and release hydrogen.

Our approach also involved using nanoparticle oxides of ZrO_2 as supports for the iron oxide. This is a novel approach since nanoparticles are normally not considered as supports for this reaction due to the high reaction temperatures. However, using nanoparticle oxide supports has significant potential as they could form mixed metal oxides with the iron and positively influence the catalytic activities.

Project Results

This project focused on the development of novel iron-based catalysts for the two-step thermochemical splitting of water into hydrogen and oxygen. The thermochemical process of splitting water is particularly well-suited for the utilization of solar energy to provide the heat for the reaction and is a way to produce a renewable hydrogen fuel. As hydrogen is difficult to transport and store, producing hydrogen on site for power plants using either proton exchange membrane (PEM) fuel cells or internal combustion engines to generate electricity or for the production of chemicals, such as liquid hydrocarbon fuels, is a very attractive approach. In this project, a two-step thermochemical process was used in which water is passed over a reduced iron oxide to generate hydrogen while the oxygen is taken up by the oxygen-deficient iron oxide (Equation 1). In the second step the resulting iron oxide is heated to desorb oxygen and regenerate the oxygen-deficient iron oxide to close the catalytic cycle (Equation 2). The main objectives of the project were to develop metal oxide catalysts that I) will release oxygen at temperatures lower than 1500°C (Equation 2), while still maintaining water-splitting activity (Equation 1) and II) are stable up to the temperature necessary for the oxygen desorption step.

$$FeO_{x-1} + H_2O \rightarrow FeO_x + H_2 \qquad \text{Equation 1}$$

$$FeO_x \xrightarrow{\Delta} FeO_{x-1} + \frac{1}{2}O_2 \qquad \text{Equation 2}$$

Reactor System. As part of the proposed research, a bench scale reactor system was designed, constructed and calibrated to evaluate the various catalysts for activity in the water-splitting reaction. The system design is shown in Figure 1 below, and a picture of the completed system is presented in Figure 2.
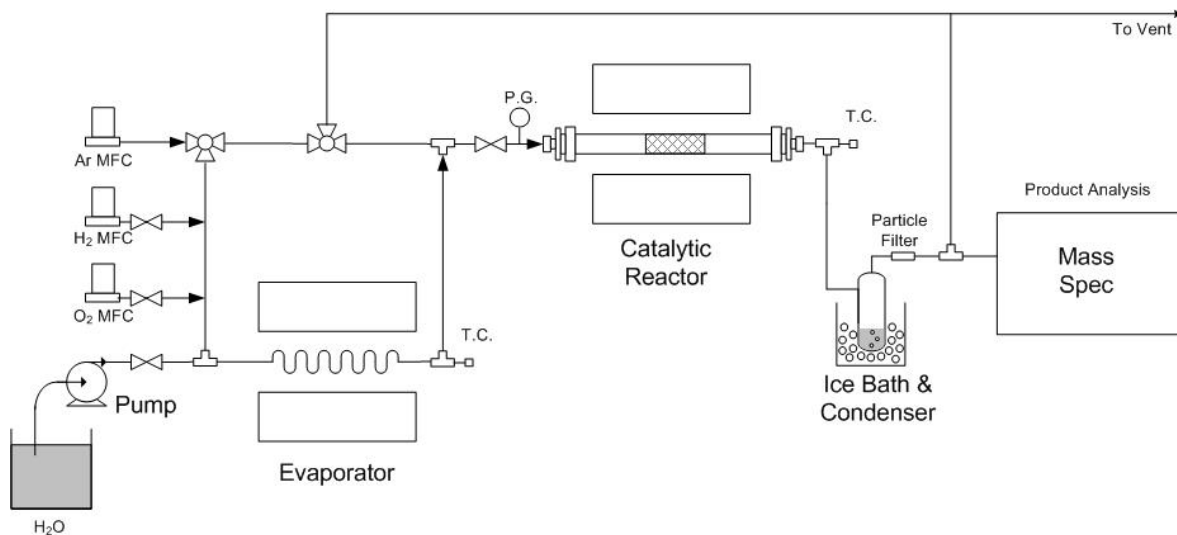

Figure 1. Flow diagram of the bench scale water-splitting reactor system.

The reactor system is configured to run both thermal reduction (Equation 2) and water splitting (Equation 1) sequentially. In the first step, the catalyst is heated in a flow of argon until the oxygen desorbs and the oxygen-deficient iron oxide is generated. This step is done at a maximum temperature of 1500 °C. When no more oxygen is generated, the reactor is switched to water-splitting mode and the temperature decreased to 1000 °C. Water is pumped into the evaporator to generate steam, which is brought to the reactor using argon as the carrier gas. The

7

steam is then decomposed over the oxygen-deficient iron oxide at 1000 °C to produce hydrogen and iron oxide. When no more hydrogen is generated, the reactor is switched back to thermal reduction mode and heated in a flow of argon to 1500 °C again to regenerate the active iron oxide species. In both steps the product gas composition is measured continuously using a mass spectrometer which is attached to the outlet of the reactor system (after the condenser to remove unreacted water). These cycles are repeated six to ten times to determine the stability of the catalysts.

The oxygen and hydrogen mass flow controllers (MFCs) in Figure 1 were used to calibrate the mass spectrometer and allow quantification of the hydrogen and oxygen in the product stream during the reaction runs.
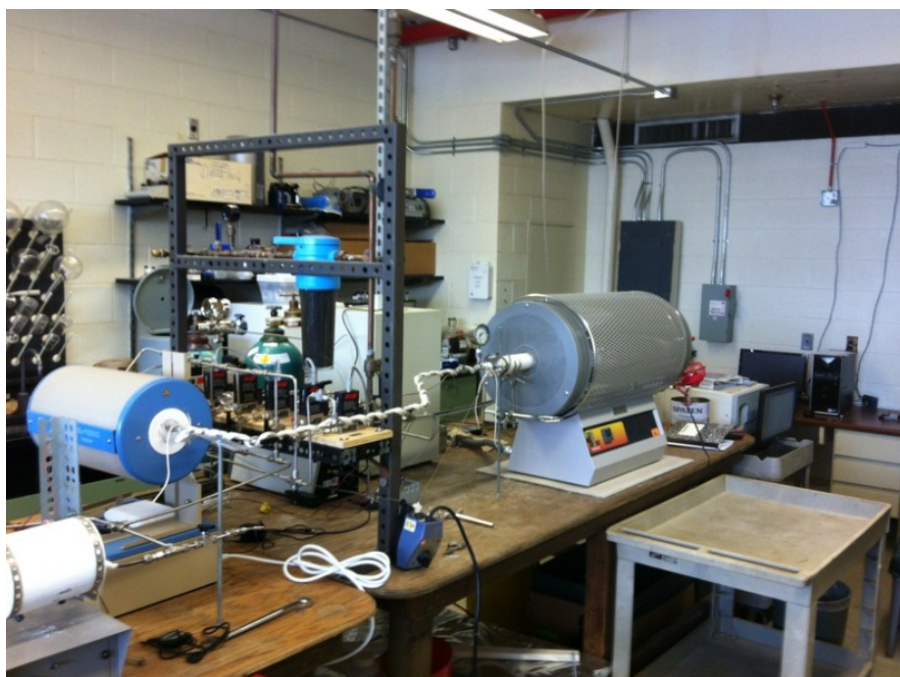

Figure 2. Completed bench scale water-splitting reactor system.

Catalyst Preparation and Evaluation. Two different iron oxide catalysts, with varying iron loading, were synthesized and tested for activity and stability in the thermochemical splitting of water. More specifically, the iron oxide was precipitated onto two commercial zirconia supports, a nanoparticle ZrO_2 (n-ZrO_2) and an yttria-stabilized zirconia with 8 mol% of yttria (8-YSZ), since zirconia is known as a high temperature ceramic. The precipitation was done by slowly adding a sodium hydroxide solution to a dispersion containing the support (either n-ZrO_2 or YSZ) and an aqueous solution of iron nitrate. The catalyst was then recovered by filtration and dried over night at 105 °C, before being heat-treated at 800 °C to decompose the iron hydroxide and form iron oxide (Fe_2O_3) on the surface of the catalysts. Before reaction, these catalysts were first thermally activated by heating to 1500 °C to generate the oxygen-deficient iron oxide, the active component in the water decomposition step. During the activation the Fe_2O_3 on the ZrO_2 is reduced to FeO (or a mixture of Fe_3O_4 and FeO), and some particle growth occurs due to the high temperatures. The oxygen evolution was monitored during this step to make sure that the reduction was complete (i.e. no more oxygen desorbed

from the catalyst) before the water-splitting step. Once the catalyst had been activated, the temperature was decreased to 1000 °C and water (steam) was introduced and the hydrogen evolution monitored (Figure 3). In this step the FeO is reoxidized to Fe_3O_4 (Equation 1). Fe_2O_3, which was present on the fresh catalyst before activation, will not form under these conditions. When no more hydrogen evolved from the catalyst, the temperature was once again increased to 1500 °C to reduce the Fe_3O_4 back to FeO (Figure 4). These steps, water splitting and thermal reduction, were repeated at least six times, as it takes a few cycles to reach a stable productivity (Figures 3 and 4).
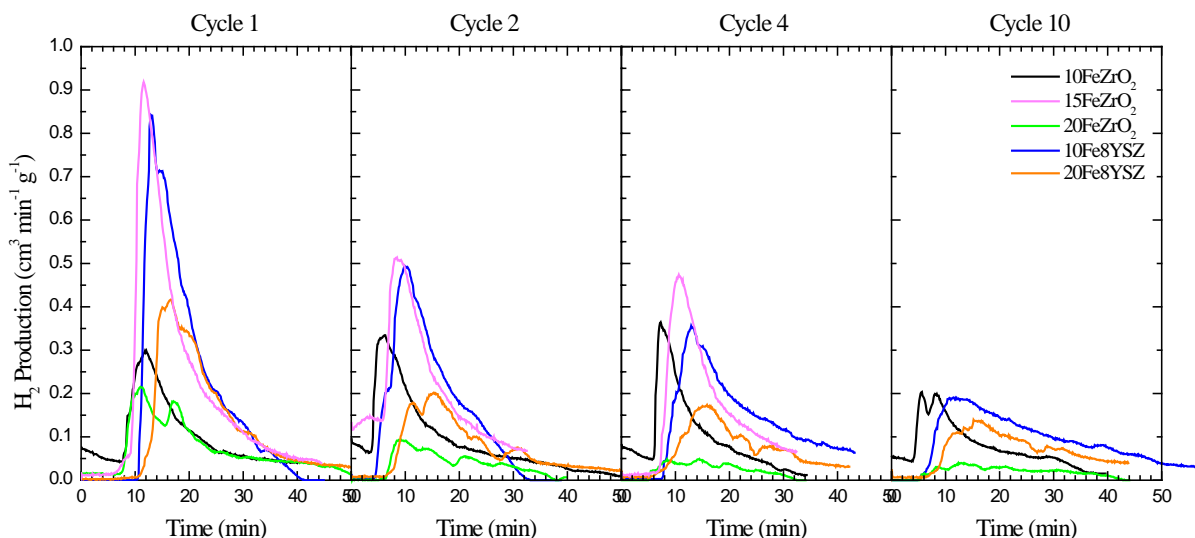

Figure 3. Hydrogen production step for cycles 1, 2, 3 and 10. ———— 10wt% $FeO_x/n-ZrO_2$, ———— 15wt% $FeO_x/n-ZrO_2$, ———— 20wt% $FeO_x/n-ZrO_2$, ———— 10wt% $FeO_x/8-YSZ$, ———— 20wt% $FeO_x/8-YSZ$.

As is evident in Figure 3, the first step generates the most hydrogen. This reveals that the catalyst is not stable after the activation step, and that further particle growth likely occurs during the second thermal reduction. The result of iron oxide particle growth is that a smaller fraction of the iron is available for reaction, i.e. a smaller fraction of the Fe_3O_4 is reduced during the thermal reduction and less FeO is then available for reaction with water. However, after the first cycle the subsequent cycles give more consistent hydrogen evolutions. This is true for all catalysts, except those with an iron content of 20 wt%. The hydrogen evolution obtained from the 20-FeO_x/ZrO_2 catalyst continues to decline with increasing number of cycles (Figure 3). This is clearly due to the fact that a smaller fraction of iron is being reduced in each cycle (figure 4). The same is true for the 20-FeO_x/YSZ catalyst, although the trend is not as severe as for the 20-FeO_x/ZrO_2 catalyst.   The highest hydrogen production is obtained over the 15 wt% FeO_x/ZrO_2 and the 10 wt% FeO_x/YSZ catalysts. The results indicate that there is an optimal iron loading on these catalysts. At low iron loadings the reaction is limited by the amount of iron present at the surface, while at higher loadings the iron is not sufficiently stabilized by the support and severe sintering occurs (see characterization section below), which reduces the available iron oxide. Comparing the iron catalysts supported on n-ZrO_2 to those supported on yttria-stabilized ZrO_2 indicates that the FeO_x/ZrO_2 catalyst is more stable than the FeO_x/YSZ catalyst, as the hydrogen evolution is more consistent over the FeO_x/ZrO_2 catalyst through ten cycles. Thus, while more hydrogen is generated during the first cycles over the FeO_x/YSZ

9

catalyst, after ten cycles the hydrogen production is very similar over the FeO_x/YSZ and FeO_x/ZrO_2 catalysts. Since the 10-FeO_x/ZrO_2 catalyst exhibited a very stable hydrogen evolution, while the 20-FeO_x/ZrO_2 catalyst showed significant deactivation even after a few cycles, a catalyst with a 15 wt% iron loading was added to the study. As is evident in both Figures 3 and 4, this catalyst shows significant promise as it has a high and stable hydrogen production, together with a stable thermal regeneration step (oxygen evolution) through four cycles.
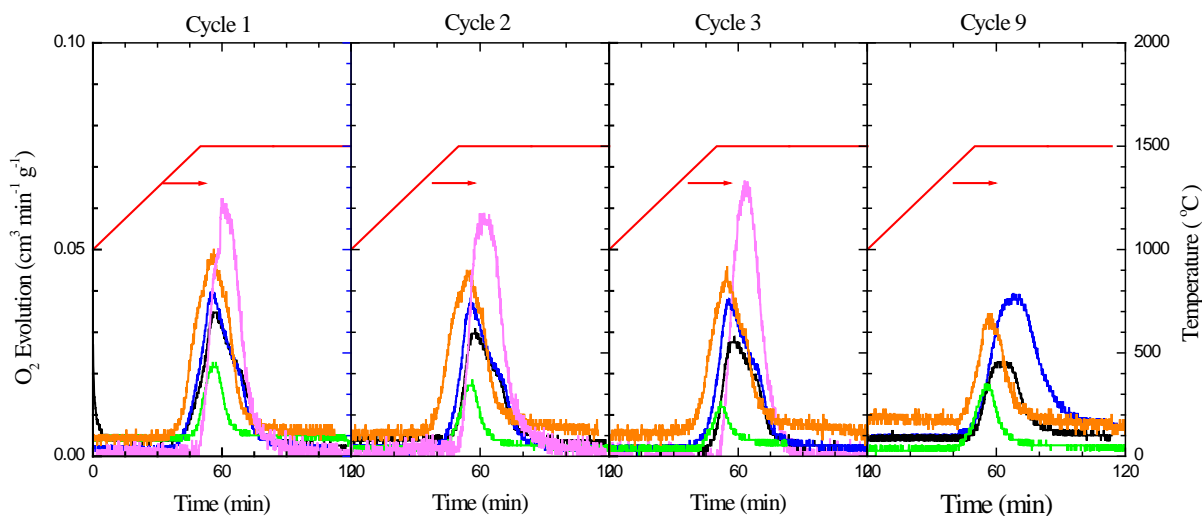

Figure 4. Thermal reduction step for cycles 1, 2, 3 and 9. ——— 10wt% FeO_x/n-ZrO_2, ——— 15wt% FeO_x/n-ZrO_2, ——— 20wt% FeO_x/n-ZrO_2, ——— 10wt% FeO_x/8-YSZ, ——— 20wt% FeO_x/8-YSZ.

Catalyst Characterization. The fresh and spent catalysts were subjected to a number of catalyst characterization techniques, such as Brunauer-Emmett-Teller (BET) surface area analysis, x-ray diffraction (XRD) measurements, and scanning electron microscopy (SEM) studies, to determine how the properties of the catalysts are altered during reaction. These measurements will help in determining the reasons for decreases in activity, and can identify important catalytic properties. Some sintering (particle growth) is observed on all of these catalysts. However, sintering at temperatures of 1500 °C can be very severe and lead to complete activity loss due to particle growth which results in a single sintered block of material. Most of the catalysts in this study were still in powder form after the ten consecutive cycles of water decomposition and thermal regeneration (Figure 5).

Figure 5. Spent FeO_x/n-ZrO_2 catalyst after 10 cycles.

The BET surface areas for fresh and spent catalysts are presented in Table 1. The fresh catalysts all have surface areas of approximately 10 m^2/g. Evidently, the catalysts with an iron loading of 20% have lower surface areas (6-8 m^2/g) compared with the 10 wt% Fe catalysts (10-

12 m^2/g), which indicates that the added iron block some of the pores in the support. The surface areas of the catalysts after reaction are an order of magnitude lower than before reaction. A lower surface area is expected due to sintering at the high temperatures of reaction. However, the data reveal that the catalysts are not completely destroyed during reaction.

Table 1. BET specific surface area measurements for select catalysts before (fresh) and after (spent) ten reaction cycles.

Catalyst	Fresh (m^2/g)	Spent (m^2/g)
10-Fe/n-ZrO$_2$	10.0	1.6
20-Fe/n-ZrO$_2$	7.8	0.7
10-Fe/8-YSZ	12.2	1.5
20-Fe/8-YSZ	6.3	0.79

The surface area is an important catalyst property, as it gives an indication of the surface area available for reaction. The smaller surface area of the 20 wt% Fe catalysts is consistent with the lower activity of these catalysts compared with the 10 wt% Fe catalysts. However, the differences in fresh (or spent) surface areas between the 10-Fe/n-ZrO$_2$ and 10-Fe/8-YSZ cannot explain the differences in behavior of these catalysts. Thus properties other than the BET surface area are also important.

The catalysts were subjected to XRD measurements, and the XRD patterns are shown in Figure 6. The XRD spectra clearly reveal that the crystal phase of ZrO$_2$ is different in the n-ZrO$_2$ and the YSZ. The nanoparticle ZrO$_2$ is monoclinic, while the yttria-stabilized zirconia is cubic (Figure 6). As expected the iron is present as Fe$_2$O$_3$ on the fresh catalysts, and the particle size is smaller on the catalysts with a 10 wt% iron loading compared to those with a 20 wt% iron loading. The larger size of the particles is evident in the XRD patterns as peaks with higher peak intensities. The XRD data reveal that the catalysts supported on YSZ behave differently from those supported on the nanoparticles ZrO$_2$. The peaks due to the monoclinic ZrO$_2$ are not significantly affected by exposure to the reaction conditions during the ten cycles.

Figure 6. XRD spectra obtained from iron oxide precipitated on n-ZrO$_2$ and 8-YSZ. $\triangledown$ ZrO$_2$ (monoclinic), $\blacktriangledown$ YSZ (cubic), $\circ$ Fe$_2$O$_3$, $\bullet$ Fe$_3$O$_4$.

In contrast, significant particle growth is observed for the YSZ support (as is evident in cubic

11

zirconia peaks with a higher intensity after reaction). The iron on the FeO_x-ZrO_2 catalysts is reduced to Fe_3O_4 after the water-splitting step, while no features due to iron oxide is detected in the XRD pattern obtained from the FeO_x/8-YSZ after the reaction cycles. This indicates that the iron oxide is incorporated into the lattice of the YSZ, which has been observed previously.[1] The increase in particle size of the YSZ support may explain why this catalyst is not stable and exhibit a continuous decline in the hydrogen production with increasing reaction cycles.

SEM images were also obtained from fresh and spent FeO_x/ZrO_2 and FeO_x/8-YSZ catalysts with a 10 wt% iron loading (Figures 7). The particle growth due to sintering is evident for both catalysts when comparing the fresh and spent catalysts. The fresh catalysts contain significantly smaller particles on the surface compared with the spent catalysts. The difference between the nanoparticle ZrO_2 and the YSZ support is also evident in the SEM images. Consistent with the BET and XRD data, the FeO_x/8-YSZ catalyst exhibit a more significant particle size increase compared with the FeO_x/ZrO_2 catalyst. The energy dispersive spectroscopy (EDS) line scans and mapping confirm the presence of iron, oxygen, zirconium, and yttrium (for the YSZ support) on the surface with iron present across large portions of the surfaces for both catalysts. EDS confirms that after the reaction cycles YSZ and zirconia are now predominantly found on the catalysts surfaces but iron can be identified by differences in geometries between the catalyst support and the iron (Figure 8).
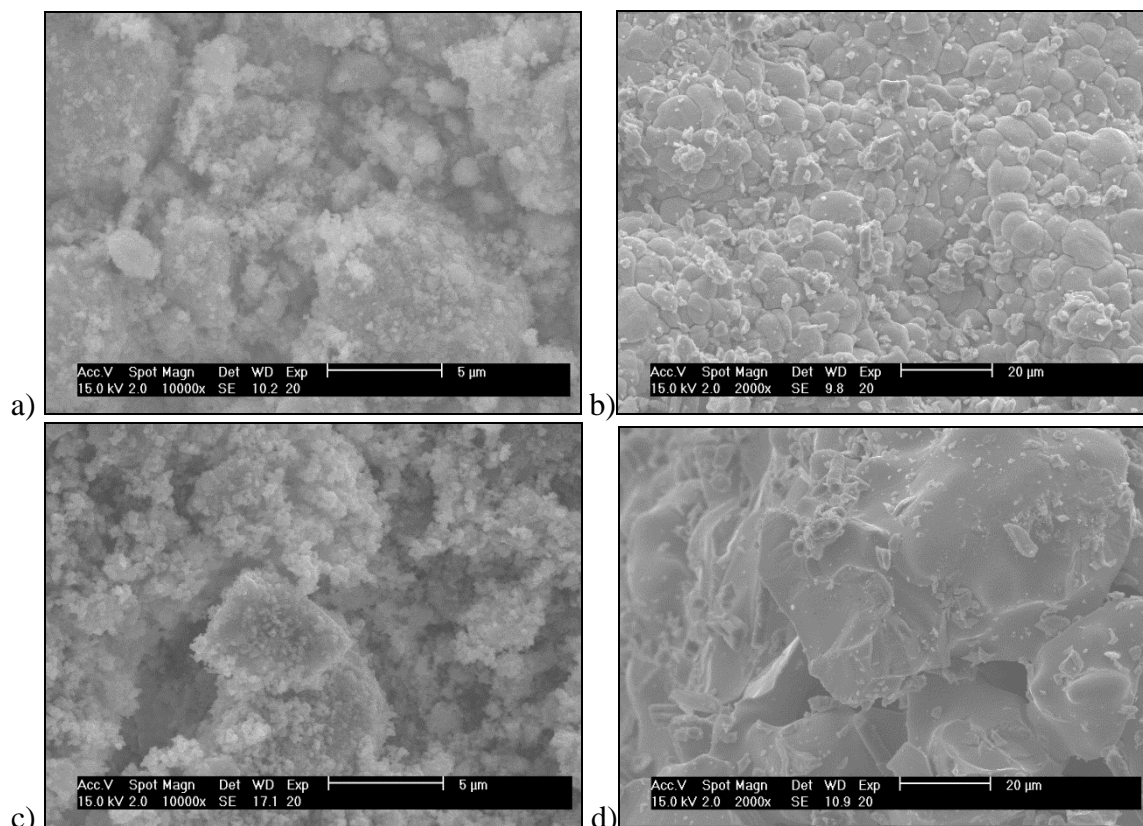

Figure 7. SEM images of fresh (a) and spent (b) 10wt% FeO_x/n-ZrO_2 and fresh (c) and spent (d) 10wt% FeO_x/8-YSZ.

[1] N. Gokon, T. Hasegawa, S. Takahashi, T. Kodama, "Thermochemical two-step water-splitting for hydrogen production using Fe-YSZ particles and a ceramic foam device," Energy 33 (2008) 1407-1416.
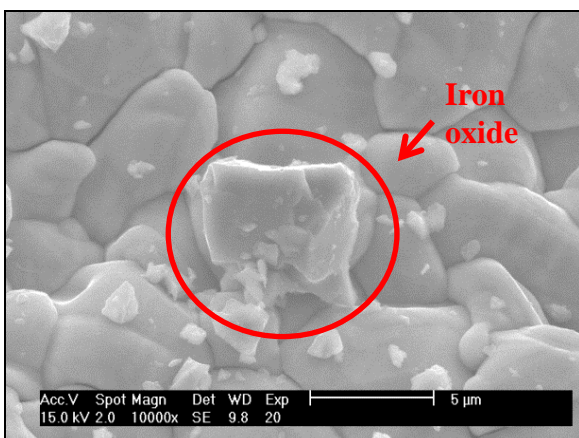
Figure 8. SEM image obtained from spent 10wt% FeO_x/ n-ZrO_2. An EDS line scan was done over this section of catalyst to identify the iron oxide particle shown in the figure.

Concluding Remarks

The iron oxide supported on zirconia is a promising catalyst combination for the thermochemical splitting of water. Future research will look into the addition of other components and other catalyst preparation methods to determine the factors of importance for stable and active catalysts under the thermochemical water splitting conditions.

Patents: N/A (not applicable)

Publications: First manuscript is in preparation based on the results in the reports.

Attachments: None.